Clinical Study

Oncology

Oncology 2014;87(suppl 1):63–72
DOI: 10.1159/000368147

Published online: November 22, 2014

Noninvasive Diagnosis of Liver Fibrosis: Utility of Data Mining of Both Ultrasound Elastography and Serological Findings to Construct a Decision Tree

Norihisa Yada[a] Masatoshi Kudo[a] Norifumi Kawada[b] Shuichi Sato[c] Yukio Osaki[d] Akihisa Ishikawa[e] Hisaaki Miyoshi[f] Michiie Sakamoto[g] Masayoshi Kage[h] Osamu Nakashima[i] Akiko Tonomura[j]

[a]Department of Gastroenterology and Hepatology, Kinki University School of Medicine, Osaka-Sayama, [b]Department of Hepatology, Graduate School of Medicine, Osaka City University, Osaka, [c]Department of Internal Medicine II, Shimane University School of Medicine, Shimane, [d]Department of Gastroenterology and Hepatology, Osaka Red Cross Hospital, Osaka, [e]Department of Internal Medicine, Hitachi General Hospital, Hitachi, [f]Department of Gastroenterology and Neurology, Faculty of Medicine, Kagawa University, Kagawa, [g]Department of Pathology, School of Medicine, Keio University, Tokyo, Departments of [h]Diagnostic Pathology and [i]Pathology, Kurume University School of Medicine, Kurume, and [j]Engineering R&D Department 1, Hitachi Aloka Medical, Ltd., Tokyo, Japan

Key Words

Data mining · Liver fibrosis · Liver fibrosis index · Real-time tissue elastography · Strain elastography

Abstract

Objective: Although liver biopsy is the gold standard for viral liver disease management, it is invasive and the sampling error rate is problematic. Real-time tissue elastography (RTE), a recently developed method of ultrasound elastography, can be used to assess liver fibrosis noninvasively but the overlap between fibrosis stages limits its ability to assess liver fibrosis adequately when used alone. ***Methods:*** A multicenter collaborative study involving 542 patients with chronic viral hepatitis and cirrhosis who were scheduled to undergo liver biopsy compared the image features obtained from RTE image analysis, the liver fibrosis index (LFI), and pathological diagnosis. RTE and a blood test were performed on the same day as the liver biopsy. Data mining was also performed to construct a decision tree, and its diagnostic performance for assessing liver fibrosis was evaluated. ***Results:*** The LFI was higher in patients with chronic hepatitis C (CHC) than in those with chronic hepatitis B (CHB). When a decision tree was constructed by data mining of RTE and serological findings, the diagnostic accuracy was very high for all fibrosis stages, with respective rates at F1, F2, F3, and F4 of 94.4, 54.1, 38.7, and 81.3% for patients with CHC and of 97.1, 50.0, 43.8, and 80.6% for patients with CHB. ***Conclusions:*** The variation in LFI values between the different etiologies appears to reflect the difference in the development style of liver fibrosis. The decision tree for assessing liver fibrosis constructed by data mining of both RTE and serological findings had a high diagnostic performance in assessing liver fibrosis and shows promising clinical utility.

KARGER

E-Mail karger@karger.com
www.karger.com/ocl

0030–2414/14/0877–0063$39.50/0

Prof. Masatoshi Kudo
Department of Gastroenterology and Hepatology
Kinki University School of Medicine
377-2 Ohno-Higashi, Osaka-Sayama, Osaka 589-8511 (Japan)
E-Mail m-kudo@med.kindai.ac.jp

Introduction

Spontaneous clearance of hepatitis C virus (HCV) almost never occurs once the infection has become chronic, so liver fibrosis progresses year after year and ultimately leads to cirrhosis in individuals with chronic hepatitis C (CHC) if they do not undergo antiviral therapy with agents such as interferons [1]. Viral hepatitis is a cause of hepatocarcinogenesis, and the incidence of liver cancer significantly increases as liver fibrosis progresses in CHC [2]. It is expected that the surveillance of liver cancer will improve detection rates of early-stage liver cancer and consequently improve prognosis through treatment, including local therapy, hepatectomy, and liver transplantation [3–9]. Liver fibrosis affects both the virus eradication rate and prognosis. Assessing liver fibrosis is therefore useful for determining the indication of treatment for viral hepatitis and predicting the risk of hepatocarcinogenesis, making it very important in clinical practice.

Liver biopsy is regarded as the gold standard for assessing liver fibrosis; however, it is an invasive technique that carries risks of bleeding and pain. Moreover, the biopsy sample evaluated is small, representing only 1/50,000 of the liver, so differences in assessment findings can arise depending on the site biopsied or the examining pathologist's judgment. One study that compared the pathological findings of liver biopsy with those of hepatectomy found a variation rate of approximately 30% [10].

Another useful assessment technique is ultrasound elastography, which noninvasively measures liver stiffness. Although liver stiffness is influenced by factors such as liver fibrosis and inflammation, it is correlated with the incidence of viral hepatocarcinogenesis, and studies have shown that the FibroScan is useful for the surveillance of liver cancer [5, 11–13]. Real-time tissue elastography (RTE), an ultrasound elastography with another measurement principle, noninvasively depicts the distortion in liver tissue caused by beating of the heart in real time; as liver fibrosis progresses, the percentage of blue low-strain areas and the textural disorganization increase [14, 15]. A verification study using a mechanical model of liver fibrosis suggested that changes in RTE images associated with the progression of liver fibrosis are seen because RTE is actually depicting liver fibrosis itself [16]. In addition, the liver fibrosis index (LFI), which is a multiple regression equation for assessing liver fibrosis using liver fibrosis estimates based on biopsy and RTE data obtained from patients with CHC and cirrhosis, is widely used as a technique for assessing liver fibrosis with RTE as it can be easily measured with RTE systems [17–20]. However, the LFI was developed based on data from patients with CHC and cirrhosis, and its usefulness for other etiologies has not been sufficiently discussed. Furthermore, the stage of fibrosis is often not completely clear when using the LFI in clinical practice, due to the large amount of overlap between the stages, so an assessment method with greater diagnostic accuracy is needed.

Against this background, in this study we examined differences between patients with CHC and chronic hepatitis B (CHB) by comparing image features from RTE image analysis, the LFI, and serological tests. We also constructed a decision tree by data mining both RTE and serological findings and evaluated its diagnostic performance for assessing liver fibrosis.

Patients and Methods

Patients

This was a multicenter collaborative study conducted at Kinki University Hospital, Osaka City University Hospital, Shimane University Hospital, Osaka Red Cross Hospital, Hitachi General Hospital, Kagawa University Hospital, Minami Wakayama Medical Center, Kumamoto Shinto General Hospital, Nagoya City University Hospital, Wakayama Medical University Hospital, Osaka Medical Center for Cancer and Cardiovascular Diseases, Ehime University Hospital, Takamatsu Red Cross Hospital, Tottori University Hospital, Yashiro General Hospital, Hyogo College of Medicine Hospital, and PL Hospital. Only patients chronically infected with either HCV or hepatitis B virus (HBV) were included (coinfected patients were excluded). The strain of hepatitis virus was determined based on whether a positive result was obtained when HCV-RNA and HBV-DNA were measured. Furthermore, patients who consumed ≥20 g of alcohol per day or had another type of chronic hepatitis such as primary biliary cirrhosis or autoimmune hepatitis were excluded. The study protocol conformed to the Declaration of Helsinki and was approved by the ethics committee of each participating institute. Informed consent to participate in the study was obtained from each patient.

Clinical and Laboratory Assessments

A blood test and RTE were performed on the same day as the liver biopsy. Aspartate aminotransferase (AST), alanine aminotransferase (ALT), gamma-glutamyl transpeptidase (GGT), total bilirubin (T-Bil), platelet count (PLT), prothrombin time (PT), international normalized ratio (INR), hyaluronic acid (HA), type IV collagen, type IV collagen 7S domain, type III procollagen N-peptide (P3P), and matrix metalloproteinase-3 (MMP3) were assessed using automated methods.

Histological Assessment

Percutaneous ultrasound-guided liver biopsy was performed on the right lobe with a Tru-Cut semiautomatic 16- or 18-gauge needle apparatus. The liver biopsy specimens were fixed in for-

malin, embedded in paraffin, and stained with hematoxylin and eosin, Masson's trichrome or Azan. All biopsy specimens were examined by 3 liver pathology experts who were blinded to the patient characteristics. Liver fibrosis was scored by the new Inuyama classification, the Japanese criteria for the histological assessment of chronic viral hepatitis [21]. The 3 pathologists assessed each case separately and differences in judgments were resolved by consensus. The stage of fibrosis was classified as follows: F0 = no fibrosis; F1 = fibrosis portal expansion; F2 = bridging fibrosis (portal-portal or portal-central linkage); F3 = bridging fibrosis with lobular distortion (disorganization), or F4 = cirrhosis.

Real-Time Tissue Elastography

The principle of RTE has been already reported by us [14, 15, 18–20, 22, 23]. Briefly, RTE was performed using ultrasonography (EUS-8500, HI-VISION 900, and HI-VISION Ascendus; Hitachi Aloka Medical, Tokyo, Japan) and the EUP-L52 linear probe (3–7 MHz; Hitachi Aloka Medical). Patients were examined in the spine position with the right arm in maximal abduction and were instructed to hold their breath. The examinations were performed on the right lobe through the intercostal spaces, with the transducer held firmly with no compression applied to the skin. The B-mode and static image superimposed on B-mode were both visualized in real time, enabling the optimal position to be easily selected. The region of interest of the strain image was 2.5 cm^2 and located about 1 cm below the surface of the liver. In addition, to obtain good images, scanning was performed to avoid large vessels and attenuation by the lungs and ribs. Videos comprising stable RTE images over ≥5 sequential heartbeats were saved 3 times. A reader blinded to patient characteristics selected 10 appropriate images from the saved videos using the electrocardiogram and strain graph as references and analyzed those images. As RTE is a technique for depicting relative strain, artifacts within the region of interest affect the results and therefore the reader selected images with few artifacts and then analyzed the areas without artifacts in these images. From each RTE image, 11 image features were extracted: mean relative strain value (MEAN); standard deviation of relative strain value (SD); percentage of low strain area (percentage of the blue colored area; %AREA); complexity of low strain area (calculated as square of perimeter divided by area; COM); skewness (SKEW); kurtosis (KURT); contrast (CON); entropy (ENT); textural complexity, inverse difference moment (IDM); angular second moment (ASM), and correlation (COR). LFI was calculated using a previously reported method [17–19].

Statistical Analysis

Descriptive statistics are shown as median and quartile, or percentage as appropriate. Differences in findings by etiology were evaluated using the nonparametric Mann-Whitney U test. Differences in findings by fibrosis stage were evaluated by multiple comparisons with Tukey's honestly significant difference test and trend analysis with the Jonckheere-Terpstra trend test. Differences were considered statistically significant at $p < 0.05$. The diagnostic performance for liver fibrosis was determined in terms of sensitivity, specificity, positive predictive value, negative predictive value, diagnostic accuracy, and area under the receiver operating characteristic curve (AUROC). All analyses were performed using SPSS Statistics 20 (IBM, Armonk, N.Y., USA).

Results

Demographics and Baseline Features

A total of 542 patients with good RTE images, good samples from liver biopsy, and with liver fibrosis were included in the analysis. The pathological diagnosis was HCV in 414 patients (F1: 179, F2: 98, F3: 62, and F4: 75) and HBV in 128 patients (F1: 69, F2: 12, F3: 16, and F4: 31).

Comparison of Serological Markers and Pathological Diagnosis

In the HCV-infected patients, as the stage of fibrosis progressed, a significant increasing trend was seen for AST, ALT, GGT, T-Bil, INR, HA, type IV collagen, type IV collagen 7S, and P3P ($p < 0.0001$), a significant decreasing trend was seen for PLT ($p < 0.0001$), and no significant trend was seen for MMP3 ($p = 0.565$). In the HBV-infected patients, as the stage of fibrosis progressed, a significant increasing trend was seen for GGT, INR, HA, type IV collagen, and type IV collagen 7S ($p < 0.0001$), a significant decreasing trend was seen for PLT ($p < 0.0001$), and no significant trend was seen for AST, ALT, T-Bil, P3P, and MMP3 ($p = 0.565$) (tables 1, 2).

Relationship between Liver Fibrosis Stage, RTE Image Features and LFI

As the stage of fibrosis progressed in the HCV-infected patients, a significant decreasing trend was seen for MEAN ($p < 0.0001$), a significant increasing trend was seen for SD, AREA, COM, CON, and SKEW ($p < 0.0001$), and no significant trend was seen for ASM, COR, ENT, IDM, and KURT. As the stage of fibrosis progressed in the HBV-infected patients, a significant decreasing trend was seen for MEAN ($p < 0.0001$), a significant increasing trend was seen for SD, AREA, COM, CON, and SKEW ($p < 0.0001$) as well as for KURT ($p = 0.001$), and no significant trend was seen for ASM, COR, ENT, and IDM.

A significant increasing trend was seen for the LFI in both HCV- and HBV-infected patients ($p < 0.0001$). Multiple comparisons between stages of fibrosis revealed a significant difference in the LFI between all stages of fibrosis in HCV-infected patients (F1 vs. F2, F1 vs. F3, F1 vs. F4, F2 vs. F3, F2 vs. F4, and F3 vs. F4). In HBV-infected patients, however, the only significant differences were between F1/F4 and F2/F4 (table 3).

Comparison of the LFI between HCV and HBV

When the LFI was compared between HCV- and HBV-infected patients at each stage of fibrosis, it was

Oncology 2014;87(suppl 1):63–72
DOI: 10.1159/000368147

Oncology 2014;87(suppl 1):63–72
DOI: 10.1159/000368147

Table 1. Comparison of serological markers and pathological fibrosis diagnosis

	HCV				p value	HBV				p value
	F1 (n = 179)	F2 (n = 98)	F3 (n = 62)	F4 (n = 75)		F1 (n = 69)	F2 (n = 12)	F3 (n = 16)	F4 (n = 31)	
Serum markers										
AST, IU/ml	33.0 (24.0, 51.0)	46.0 (30.0, 71.0)	66.5 (45.3, 111.0)	59.0 (44.0, 89.0)	<0.0001	33.0 (23.0, 58.5)	51.0 (21.0, 138.0)	43.5 (26.3, 80.0)	36.0 (25.3, 45.8)	0.619
ALT, IU/ml	38.0 (24.0, 56.0)	51.0 (29.0, 92.0)	66.5 (45.3, 117.0)	52.0 (32.0, 94.0)	<0.0001	34.0 (19.0, 110.0)	93.0 (23.0, 165.0)	58.5 (22.0, 74.3)	31.5 (17.8, 46.8)	0.315
GGT, IU/ml	29.0 (19.0, 57.0)	37.0 (22.0, 65.0)	43.5 (29.0, 69.5)	43.0 (25.0, 62.0)	<0.0001	26.0 (16.0, 46.5)	35.0 (18.0, 40.0)	57.0 (36.0, 89.8)	42.5 (26.5, 120.0)	<0.0001
T-Bil, mg/dl	0.70 (0.05, 0.90)	0.70 (0.50, 0.90)	0.75 (0.60, 1.08)	0.90 (0.70, 1.45)	<0.0001	0.60 (0.50, 0.85)	0.70 (0.60, 0.80)	0.70 (0.53, 0.98)	0.90 (0.60, 1.70)	0.005
PLT	19.4 (15.3, 22.2)	16.5 (12.3, 19.7)	12.8 (9.53, 16.2)	9.2 (6.6, 12.7)	<0.0001	20.4 (16.5, 26.9)	18.0 (15.1, 19.8)	15.6 (14.3, 19.8)	10.7 (7.8, 15.1)	<0.0001
INR	0.98 (0.94, 1.02)	1.02 (0.96, 1.06)	1.07 (1.01, 1.11)	1.14 (1.08, 1.23)	<0.0001	1.02 (0.99, 1.06)	1.06 (0.98, 1.10)	1.05 (0.99, 1.13)	1.10 (1.02, 1.14)	<0.0001
HA, ng/ml	38.0 (25.2, 75.8)	71.0 (41.0, 115.0)	233.2 (89.0, 413.0)	314.1 (170.8, 513.3)	<0.0001	26.8 (19.3, 45.1)	39.0 (25.0, 90.0)	87.1 (34.8, 148.0)	109.5 (83.2, 193.3)	<0.0001
Collagen type, ng/ml										
IV	116.0 (93.5, 145.5)	126.0 (96.5, 158.0)	181.0 (141.3, 232.0)	246.0 (174.0, 312.0)	<0.0001	104.0 (90.0, 125.5)	124.0 (79.3, 155.8)	153.5 (100.3, 224.8)	171.0 (119.0, 193.0)	<0.0001
IV 7S	4.4 (3.7, 5.2)	5.3 (4.4, 6.1)	7.2 (5.7, 8.9)	8.6 (7.0, 11.0)	<0.0001	4.0 (3.5, 4.9)	4.4 (3.8, 5.4)	5.7 (4.2, 6.7)	5.8 (5.0, 7.1)	<0.0001
P3P, U/ml	0.79 (0.66, 0.90)	0.80 (0.71, 1.00)	1.05 (0.83, 1.30)	1.10 (0.90, 1.30)	<0.0001	0.58 (0.50, 0.70)	0.84 (0.65, 0.94)	0.63 (0.48, 0.81)	0.63 (0.51, 0.77)	0.201
MMP3, ng/ml	37.7 (25.6, 58.1)	34.3 (27.0, 50.4)	40.2 (24.6, 52.7)	39.0 (32.5, 55.9)	0.565	36.7 (21.2, 46.0)	51.3 (28.0, 64.1)	62.9 (37.7, 80.7)	41.1 (28.5, 51.1)	0.152

Values are presented as median (first quartile, third quartile). The p values were calculated with the Jonckheere-Terpstra trend test.

Table 2. Comparison of serological markers and etiology

	F1		p value	F2		p value	F3		p value	F4		p value
	HCV (n = 179)	HBV (n = 69)		HCV (n = 98)	HBV (n = 12)		HCV (n = 62)	HBV (n = 16)		HCV (n = 75)	HBV (n = 31)	
Serum markers												
AST, IU/ml	33.0 (24.0, 51.0)	33.0 (23.0, 58.5)	0.941	46.0 (30.0, 71.0)	51.0 (21.0, 138.0)	0.767	66.5 (45.3, 111.0)	43.5 (26.3, 80.0)	0.049	59.0 (44.0, 89.0)	36.0 (25.3, 45.8)	0.000
ALT, IU/ml	38.0 (24.0, 56.0)	34.0 (19.0, 110.0)	0.776	51.0 (29.0, 92.0)	93.0 (23.0, 165.0)	0.497	66.5 (45.3, 117.0)	58.5 (22.0, 74.3)	0.202	52.0 (32.0, 94.0)	31.5 (17.8, 46.8)	0.000
GGT, IU/ml	29.0 (19.0, 57.0)	26.0 (16.0, 46.5)	0.110	37.0 (22.0, 65.0)	35.0 (18.0, 40.0)	0.431	43.5 (29.0, 69.5)	57.0 (36.0, 89.8)	0.263	43.0 (25.0, 62.0)	42.5 (26.5, 120.0)	0.394
T-Bil, mg/dl	0.70 (0.05, 0.90)	0.60 (0.50, 0.85)	0.694	0.70 (0.50, 0.90)	0.70 (0.60, 0.80)	0.991	0.75 (0.60, 1.08)	0.70 (0.53, 0.98)	0.891	0.90 (0.70, 1.45)	0.90 (0.60, 1.70)	0.832
PLT	19.4 (15.3, 22.2)	20.4 (16.5, 26.9)	0.030	16.5 (12.3, 19.7)	18.0 (15.1, 19.8)	0.380	12.8 (9.53, 16.2)	15.6 (14.3, 19.8)	0.056	9.2 (6.6, 12.7)	10.7 (7.8, 15.1)	0.078
INR	0.98 (0.94, 1.02)	1.02 (0.99, 1.06)	0.000	1.02 (0.96, 1.06)	1.06 (0.98, 1.10)	0.108	1.07 (1.01, 1.11)	1.05 (0.99, 1.13)	0.741	1.14 (1.08, 1.23)	1.10 (1.02, 1.14)	0.018
HA, ng/ml	38.0 (25.2, 75.8)	26.8 (19.3, 45.1)	0.002	71.0 (41.0, 115.0)	39.0 (25.0, 90.0)	0.091	233.2 (89.0, 413.0)	87.1 (34.8, 148.0)	0.016	314.1 (170.8, 513.3)	109.5 (83.2, 193.3)	0.000
Collagen type, ng/ml												
IV	116.0 (93.5, 145.5)	104.0 (90.0, 125.5)	0.136	126.0 (96.5, 158.0)	124.0 (79.3, 155.8)	0.879	181.0 (141.3, 232.0)	153.5 (100.3, 224.8)	0.331	246.0 (174.0, 312.0)	171.0 (119.0, 193.0)	0.002
IV 7S	4.4 (3.7, 5.2)	4.0 (3.5, 4.9)	0.035	5.3 (4.4, 6.1)	4.4 (3.8, 5.4)	0.123	7.2 (5.7, 8.9)	5.7 (4.2, 6.7)	0.020	8.6 (7.0, 11.0)	5.8 (5.0, 7.1)	0.000
P3P, U/ml	0.79 (0.66, 0.90)	0.58 (0.50, 0.70)	0.000	0.80 (0.71, 1.00)	0.84 (0.65, 0.94)	0.698	1.05 (0.83, 1.30)	0.63 (0.48, 0.81)	0.001	1.10 (0.90, 1.30)	0.63 (0.51, 0.77)	0.000
MMP3, ng/ml	37.7 (25.6, 58.1)	36.7 (21.2, 46.0)	0.217	34.3 (27.0, 50.4)	51.3 (28.0, 64.1)	0.177	40.2 (24.6, 52.7)	62.9 (37.7, 80.7)	0.030	39.0 (32.5, 55.9)	41.1 (28.5, 51.1)	0.542

Values are presented as median (first quartile, third quartile). The p values were calculated with the Mann-Whitney U test.

Table 3. Relationship between liver fibrosis stage, RTE image features and LFI

	HCV				p value	HBV				p value
	F1 (n = 179)	F2 (n = 98)	F3 (n = 62)	F4 (n = 75)		F1 (n = 69)	F2 (n = 12)	F3 (n = 16)	F4 (n = 31)	
RTE features										
MEAN	113.9 (107.2, 119.9)	109.6 (102.2, 115.1)	103.0 (94.8, 111.6)	93.4 (82.5, 105.0)	<0.0001	117.8 (107.4, 122.3)	119.0 (112.7, 121.8)	108.6 (103.1, 116.5)	101.4 (87.7, 109.7)	<0.0001
SD	52.3 (45.9, 58.7)	57.3 (50.6, 60.7)	59.6 (54.7, 63.4)	60.9 (57.6, 63.9)	<0.0001	49.1 (44.6, 56.9)	50.6 (44.6, 54.2)	57.3 (52.2, 61.5)	63.4 (56.9, 65.1)	<0.0001
AREA	14.2 (7.6, 20.8)	19.1 (11.8, 27.2)	25.2 (16.3, 33.7)	34.5 (22.5, 44.2)	<0.0001	11.2 (6.2, 19.2)	11.3 (6.2, 16.2)	20.6 (13.5, 27.7)	29.0 (19.8, 39.2)	<0.0001
COM	20.3 (18.5, 24.1)	22.8 (19.8, 26.2)	25.2 (21.3, 29.9)	31.3 (24.6, 40.2)	<0.0001	20.1 (18.5, 25.8)	20.7 (19.6, 21.8)	24.5 (21.3, 30.2)	28.9 (23.6, 34.5)	<0.0001
ASM	0.00025 (0.00019, 0.00035)	0.00020 (0.00017, 0.00032)	0.000212 (0.000178, 0.000315)	0.000294 (0.000190, 0.000453)	0.983	0.000209 (0.000183, 0.000268)	0.000196 (0.000170, 0.000220)	0.000177 (0.000175, 0.000188)	0.000213 (0.000177, 0.000285)	0.159
CON	229.6 (173.4, 268.6)	250.0 (206.9, 309.0)	261.2 (213.5, 324.0)	266.7 (233.8, 320.7)	<0.0001	221.7 (18.08, 285.2)	239.1 (198.4, 283.7)	272.2 (250.7, 279.0)	294.1 (249.1, 372.2)	<0.0001
COR	0.958 (0.947, 0.965)	0.958 (0.950, 0.966)	0.957 (0.950, 0.967)	0.962 (0.951, 0.966)	0.117	0.953 (0.944, 0.959)	0.946 (0.943, 0.955)	0.956 (0.947, 0.961)	0.954 (0.945, 0.968)	0.139
ENT	3.83 (3.76, 3.87)	3.85 (3.80, 3.89)	3.86 (3.81, 3.89)	3.84 (3.76, 3.88)	0.052	3.81 (3.74, 3.86)	3.80 (3.77, 3.86)	3.86 (3.84, 3.88)	3.84 (3.80, 3.89)	0.024
IDM	0.110 (0.095, 0.122)	0.101 (0.091, 0.117)	0.096 (0.091, 0.118)	0.108 (0.093, 0.122)	0.154	0.100 (0.091, 0.111)	0.092 (0.088, 0.100)	0.092 (0.089, 0.095)	0.100 (0.087, 0.106)	0.147
SKEW	0.199 (0.071, 0.300)	0.253 (0.122, 0.361)	0.332 (0.178, 0.461)	0.429 (0.321, 0.679)	<0.0001	0.116 (−0.517, 0.260)	0.124 (0.025, 0.219)	0.236 (0.178, 0.289)	0.376 (0.213, 0.540)	<0.0001
KURT	2.38 (2.24, 2.57)	2.34 (2.22, 2.48)	2.29 (2.20, 2.40)	2.34 (2.23, 2.64)	0.334	2.49 (2.31, 2.68)	2.48 (2.31, 2.63)	2.33 (2.29, 2.43)	2.33 (2.19, 2.47)	0.001
LFI	1.81 (1.41, 2.22)	2.10 (1.67, 2.56)	2.47 (1.97, 2.88)	2.97 (2.41, 3.45)	<0.0001	1.52 (1.16, 2.06)	1.61 (1.31, 1.84)	2.16 (1.66, 2.58)	2.66 (2.15, 3.13)	<0.0001

Values are presented as median (first quartile, third quartile). The p values were calculated with the Jonckheere-Terpstra trend test.

Oncology 2014;87(suppl 1):63–72
DOI: 10.1159/000368147

Table 4. Relationship between etiology, RTE image features and LFI

	F1		p value	F2		p value	F3		p value	F4		p value
	HCV (n = 179)	HBV (n = 69)		HCV (n = 98)	HBV (n = 12)		HCV (n = 62)	HBV (n = 16)		HCV (n = 75)	HBV (n = 31)	
RTE features												
MEAN	113.9 (107.2, 119.9)	117.8 (107.4, 122.3)	0.012	109.6 (102.2, 115.1)	119.0 (112.7, 121.8)	0.003	103.0 (94.8, 111.6)	108.6 (103.1, 116.5)	0.033	93.4 (82.5, 105.0)	101.4 (87.7, 109.7)	0.057
SD	52.3 (45.9, 58.7)	49.1 (44.6, 56.9)	0.091	57.3 (50.6, 60.7)	50.6 (44.6, 54.2)	0.006	59.6 (54.7, 63.4)	57.3 (52.2, 61.5)	0.162	60.9 (57.6, 63.9)	63.4 (56.9, 65.1)	0.395
AREA	14.2 (7.6, 20.8)	11.2 (6.2, 19.2)	0.121	19.1 (11.8, 27.2)	11.3 (6.2, 16.2)	0.010	25.2 (16.3, 33.7)	20.6 (13.5, 27.7)	0.055	34.5 (22.5, 44.2)	29.0 (19.8, 39.2)	0.109
COM	20.3 (18.5, 24.1)	20.1 (18.5, 25.8)	0.985	22.8 (19.8, 26.2)	20.7 (19.6, 21.8)	0.114	25.2 (21.3, 29.9)	24.5 (21.3, 30.2)	0.757	31.3 (24.6, 40.2)	28.9 (23.6, 34.5)	0.186
ASM	0.00025 (0.00019, 0.00035)	0.000209 (0.000183, 0.000268)	0.008	0.00020 (0.00017, 0.00032)	0.000196 (0.000170, 0.000220)	0.242	0.000212 (0.000178, 0.000315)	0.000177 (0.000175, 0.000188)	0.006	0.000294 (0.000190, 0.000453)	0.000213 (0.000177, 0.000285)	0.027
CON	229.6 (173.4, 268.6)	221.7 (18.08, 285.2)	0.484	250.0 (206.9, 309.0)	239.1 (198.4, 283.7)	0.673	261.2 (213.5, 324.0)	272.2 (250.7, 279.0)	0.488	266.7 (233.8, 320.7)	294.1 (249.1, 372.2)	0.117
COR	0.958 (0.947, 0.965)	0.953 (0.944, 0.959)	0.003	0.958 (0.950, 0.966)	0.946 (0.943, 0.955)	0.004	0.957 (0.950, 0.967)	0.956 (0.947, 0.961)	0.245	0.962 (0.951, 0.966)	0.954 (0.945, 0.968)	0.534
ENT	3.83 (3.76, 3.87)	3.81 (3.74, 3.86)	0.238	3.85 (3.80, 3.89)	3.80 (3.77, 3.86)	0.153	3.86 (3.81, 3.89)	3.86 (3.84, 3.88)	0.990	3.84 (3.76, 3.88)	3.84 (3.80, 3.89)	0.629
IDM	0.110 (0.095, 0.122)	0.100 (0.091, 0.111)	0.002	0.101 (0.091, 0.117)	0.092 (0.088, 0.100)	0.071	0.096 (0.091, 0.118)	0.092 (0.089, 0.095)	0.026	0.108 (0.093, 0.122)	0.100 (0.087, 0.106)	0.019
SKEW	0.199 (0.071, 0.300)	0.116 (−0.517, 0.260)	0.015	0.253 (0.122, 0.361)	0.124 (0.025, 0.219)	0.039	0.332 (0.178, 0.461)	0.236 (0.178, 0.289)	0.065	0.429 (0.321, 0.679)	0.376 (0.213, 0.540)	0.083
KURT	2.38 (2.24, 2.57)	2.49 (2.31, 2.68)	0.005	2.34 (2.22, 2.48)	2.48 (2.31, 2.63)	0.034	2.29 (2.20, 2.40)	2.33 (2.29, 2.43)	0.158	2.34 (2.23, 2.64)	2.33 (2.19, 2.47)	0.200
LFI	1.81 (1.41, 2.22)	1.52 (1.16, 2.06)	0.029	2.10 (1.67, 2.56)	1.61 (1.31, 1.84)	0.010	2.47 (1.97, 2.88)	2.16 (1.66, 2.58)	0.051	2.97 (2.41, 3.45)	2.66 (2.15, 3.13)	0.042

Values are presented as median (first quartile, third quartile). The p values were calculated with the Mann-Whitney U test.

Table 5. Diagnostic performance of the LFI for liver fibrosis assessment

	HCV			HBV		
	F4	>F3	>F2	F4	>F3	>F2
AUROC	0.803	0.774	0.73	0.821	0.806	0.744
Cutoff	2.45	2.42	2.31	2.07	1.94	1.91
Positive predictive value	37.8	58.2	58.7	80.6	78.7	66.1
Negative predictive value	92.9	81.6	79.9	71.1	75.3	72.5
Intensity	74.7	65	79.3	47.2	64.9	67.2
Specificity	72.9	76.9	59.6	92	85.9	71.4
Accuracy	73.2	72.2	67.9	73.4	76.6	69.5

found to be significantly higher in HCV-infected patients at stages F1, F2, and F4 (F1: HCV = 181, HBV = 1.52, p = 0.029; F2: HCV = 2.10, HBV = 1.61, p = 0.010; F4: HCV = 2.97, HBV = 2.66, p = 0.042) and marginally higher in HCV-infected patients at stage F3 (HCV = 2.47, HBV = 2.16, p = 0.051) (table 4).

AUROC Analysis

The LFI cutoff values for each stage of fibrosis were calculated by AUROC analysis to evaluate the diagnostic performance of the LFI for liver fibrosis assessment. In HCV-infected patients, the diagnostic accuracy was 73.2 at F4, 72.2 at ≥F3, and 67.9 at ≥F2. In HBV-infected patients, the diagnostic accuracy was 73.4 at F4, 76.6 at ≥F3, and 69.5 at ≥F2 (table 5).

Data Mining Analysis

The LFI is the numerical value calculated from HCV. Therefore, by using the LFI and the serological findings for HCV as well as the 11 feature values of RTE and the serological findings for HBV, the decision tree was calculated. The HCV decision tree, which comprises LFI, AST, ALT, GGT, T-Bil, PLT, HA, and type IV collagen, had a diagnostic accuracy of 94.4% for F1, 54.1% for F2, 38.7% for F3, and 81.3% for F4. The HBV decision tree, which comprises COM, CON, IDM, ALT, PLT, INR, and HA, had a diagnostic accuracy of 97.1% for F1, 50.0% for F2, 43.8% for F3, and 80.6% for F4 (fig. 1; table 6).

Discussion

The LFI, which is a multiple regression equation for assessing liver fibrosis using liver fibrosis estimates from biopsy and RTE image feature values obtained from patients with CHC or cirrhosis, is widely used as the primary diagnostic technique with RTE as it can easily be measured with RTE diagnostic equipment. However, few studies have examined differences in RTE images or the LFI due to differences in etiology, and the usefulness of the LFI for etiologies other than HCV has not been sufficiently discussed. In this study, we found that the LFI was significantly higher in HCV- than in HBV-infected patients with the same stage of fibrosis. This was likely influenced by differences in how fibrosis progresses in these etiologies. Specifically, HCV-infected patients develop micronodular cirrhosis, whereas HBV-infected patients develop macronodular cirrhosis. However, in criteria for evaluating pathological fibrosis in viral liver diseases (e.g., the new Inuyama classification), the stage of fibrosis is based on the area where fibrosis develops rather than the amount of fibrosis present. In essence, the amount of fibrosis per unit of area would be higher in HCV- than in HBV-infected patients with the same stage of fibrosis because the progression of HCV-related fibrosis is micronodular, thereby making the LFI higher as well. When using the LFI, the etiology of the patient must be confirmed before assessing the fibrosis stage.

Although evaluation using AUROC yields a somewhat high diagnostic accuracy for liver fibrosis assessment by the LFI, the stage of fibrosis when using LFI alone in clinical practice is often not exactly clear due to the large amount of overlap in the LFI between stages. Whereas AUROC can be used only to evaluate the diagnostic performance of assessment between two choices, namely ≥F2/F1, ≥F3/≤F2 or F4/≤F3, the decision tree can assess the exact stage of fibrosis (i.e., F1, F2, F3 or F4). Furthermore, the decision tree constructed in this study can be used to determine the specific stage of liver fibrosis based on etiology, serological findings, and RTE findings with very high diagnostic accuracy of each fibrosis stage, suggesting its utility in clinical practice as well. However, the sample size in the F2

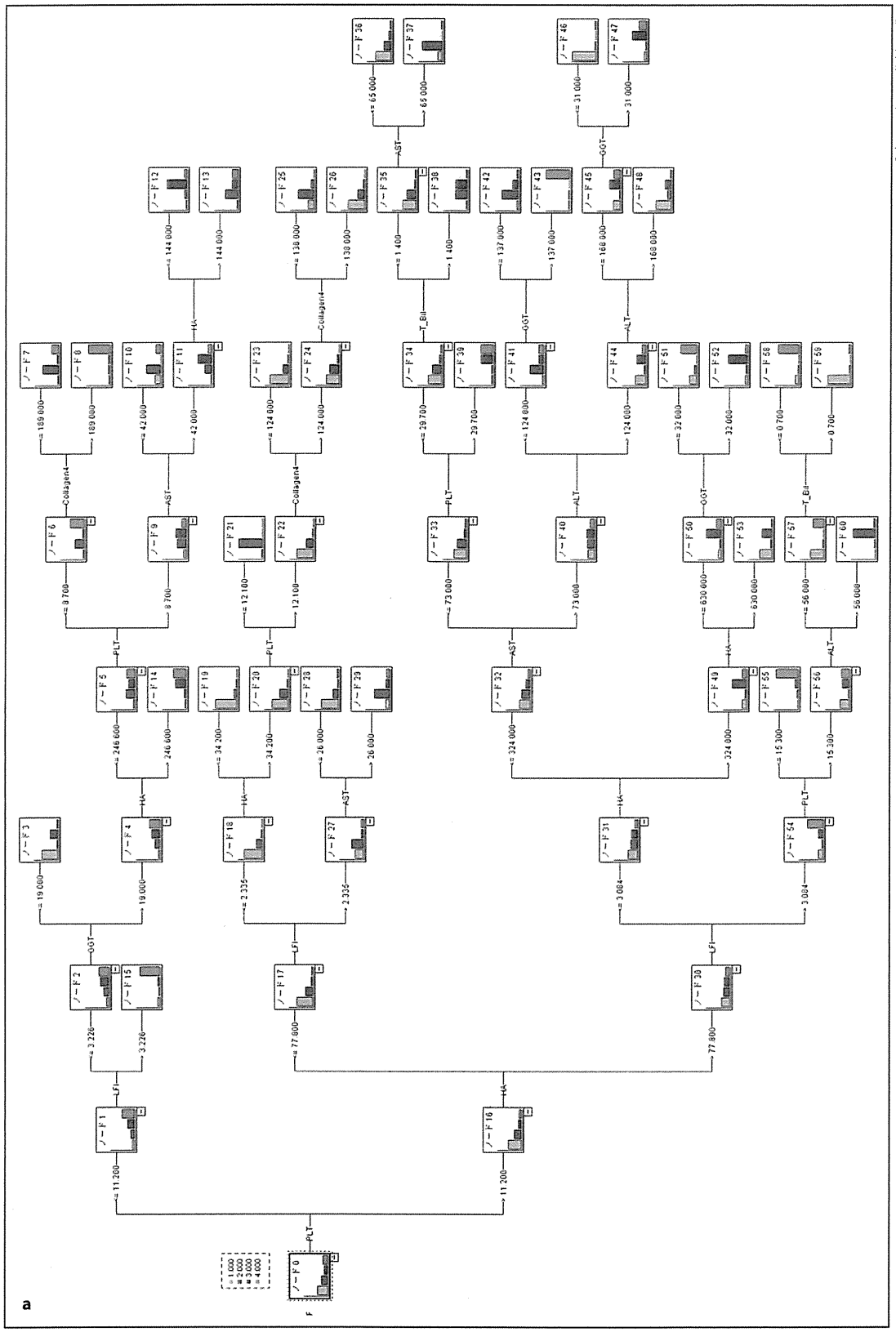

1

(For legend see next page.)

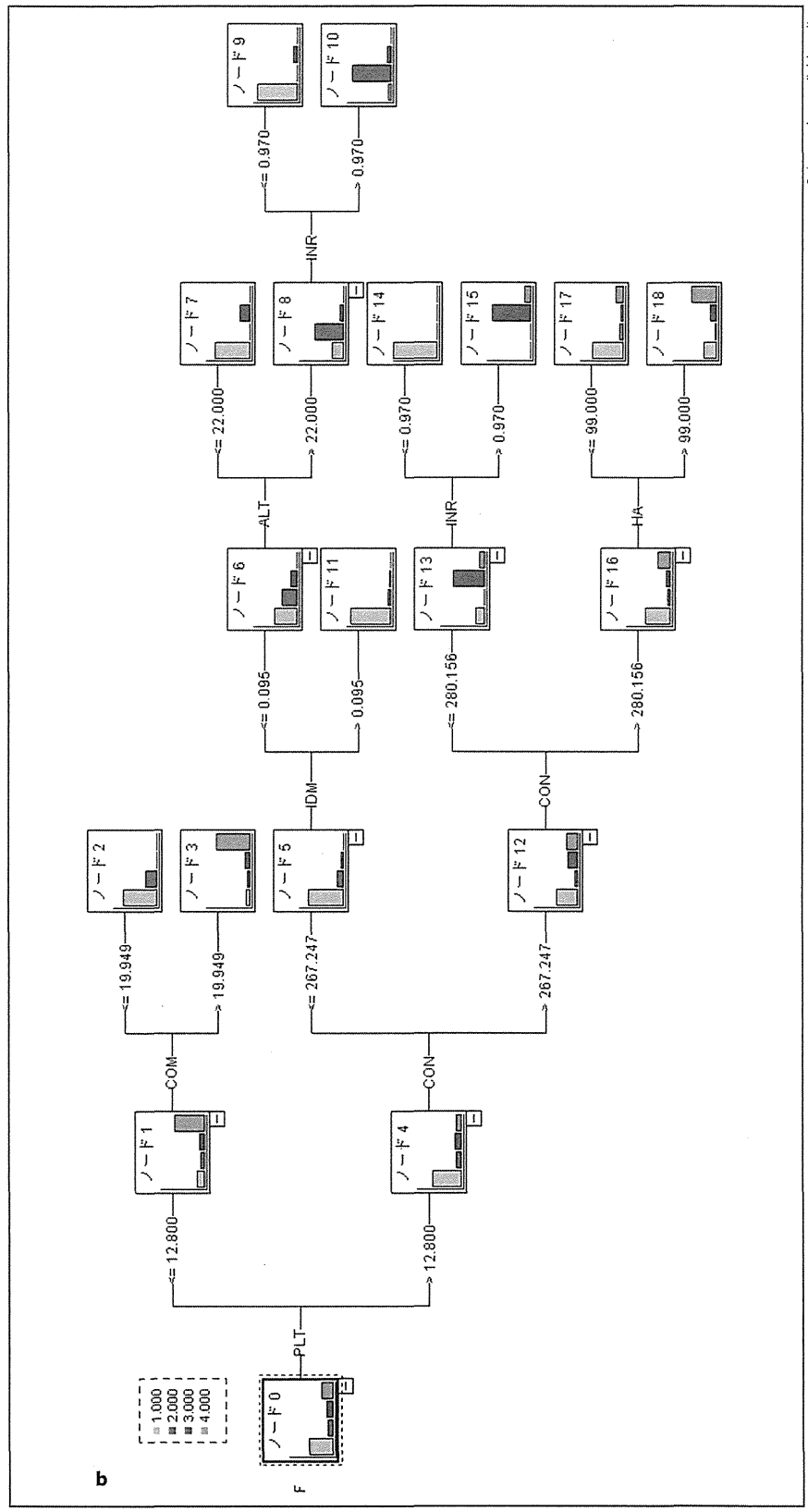

Fig. 1. Data mining for the diagnosis of the fibrosis stage in chronic viral hepatitis: fibrosis diagnosis of CHC (**a**) and CHB (**b**). Each bar graph shows the percentage of cases. The pale blue, red, blue, and green bars represent F1, F2, F3, and F4 fibrosis stage, respectively (colors refer to the online version only). T_Bil = Total bilirubin; Collagen4 = type IV collagen.

Table 6. Diagnostic performance of data mining with both ultrasound elastography and serological findings

	Data mining diagnosis							
	HCV				HBV			
	F1	F2	F3	F4	F1	F2	F3	F4
Pathological diagnosis								
F1	169 (94.4)	8 (4.5)	0	2 (1.1)	67 (97.1)	0	0	2 (2.9)
F2	42 (42.9)	53 (54.1)	1 (1.0)	2 (2.0)	5 (41.7)	6 (50)	0	1 (8.3)
F3	10 (16.1)	10 (16.1)	24 (38.7)	18 (29.0)	6 (37.5)	0	7 (43.8)	3 (18.8)
F4	3 (4.0)	6 (8.0)	5 (6.7)	61 (81.3)	5 (16.1)	0	1 (3.2)	25 (80.6)

Values are presented as n (%).

or F3 stage is too small both in HCV and HBV, which seems to be the reason of low accuracy of the F2 and F3 fibrosis stage.

In this study, we used the gold standard method of assessing liver fibrosis stage with samples obtained by liver biopsy, but, as mentioned previously, sampling error is more likely with an assessment by liver biopsy than with an assessment of hepatectomy specimens. Therefore, to construct a more accurate decision tree, it would be ideal to make the pathological diagnosis based on the hepatectomy specimens. Furthermore, it is also necessary to try to eliminate discrepancies in assessment between readers, for example, by adding computer-aided pathological diagnosis. In light of these issues, further research must be conducted to enable ultrasound elastography to be used as a tool for obtaining a more accurate diagnosis in clinical practice.

Acknowledgements

This study was supported by Health and Labour Sciences Research Grants for the Research on Hepatitis from the Japanese Ministry of Health, Labour and Welfare. The authors thank those who conducted the patient enrollment, namely Kenji Fujimoto (Division of Clinical Research and Department of Internal Medicine, Minami Wakakayama Medical Center, Tanabe, Japan), Shiho Miyase (Department of Gastroenterology and Hepatology, Kumamoto Shinto General Hospital, Kumamoto, Japan), Shunsuke Nojiri (Department of Gastroenterology and Metabolism, Nagoya City University Graduate School of Medical Sciences, Nagoya, Japan), Hideyuki Tamai (Second Department of Internal Medicine, Wakayama Medical University, Wakayama, Japan), Kazuho Imanaka (Department of Hepatobiliary and Pancreatic Oncology, Osaka Medical Center for Cancer and Cardiovascular Diseases, Osaka, Japan), Kazuyoshi Ohkawa (Department of Hepatobiliary and Pancreatic Oncology, Osaka Medical Center for Cancer and Cardiovascular Diseases, Osaka, Japan), Yoichi Hiasa (Department of Gastroenterology and Metabology, Ehime University Graduate School of Medicine, Toon, Japan), Chikara Ogawa (Department of Gastroenterology, Takamatsu Red Cross Hospital, Takamatsu, Japan), Masahiko Koda (Division of Medicine and Clinical Science, Department of Multidisciplinary Internal Medicine, Tottori University School of Medicine, Yonago, Japan), Shuichi Miyase (Department of Gastroenterology, Yatsushiro General Hospital, Yatsushiro, Japan), and Hiroko Iijima (Division of Hepatobiliary and Pancreatic Diseases, Department of Internal Medicine, Hyogo College of Medicine, Nishinomiya, Japan), and Katsuhiko Fukuda (Department of Gastroenterology, PL Hospital, Tondabayashi, Japan).

Disclosure Statement

The authors declare that no financial or other conflicts of interest exist in relation to the content of this article.

References

1 Shiratori Y, Imazeki F, Moriyama M, Yano M, Arakawa Y, Yokosuka O, Kuroki T, Nishiguchi S, Sata M, Yamada G, Fujiyama S, Yoshida H, Omata M: Histologic improvement of fibrosis in patients with hepatitis C who have sustained response to interferon therapy. Ann Intern Med 2000;132:517–524.

2 Yoshida H, Shiratori Y, Moriyama M, Arakawa Y, Ide T, Sata M, Inoue O, Yano M, Tanaka M, Fujiyama S, Nishiguchi S, Kuroki T, Imazeki F, Yokosuka O, Kinoyama S, Yamada G, Omata M: Interferon therapy reduces the risk for hepatocellular carcinoma: national surveillance program of cirrhotic and noncirrhotic patients with chronic hepatitis C in Japan. IHIT study group. Inhibition of Hepatocarcinogenesis by Interferon Therapy. Ann Intern Med 1999;131:174–181.

3 Kim DY, Han KH: Epidemiology and surveillance of hepatocellular carcinoma. Liver Cancer 2012;1:2–14.
4 Kudo M: Early hepatocellular carcinoma: definition and diagnosis. Liver Cancer 2013;2: 69–72.
5 Kudo M: Prediction of hepatocellular carcinoma incidence risk by ultrasound elastography. Liver Cancer 2014;3:1–5.
6 Belghiti J, Fuks D: Liver resection and transplantation in hepatocellular carcinoma. Liver Cancer 2012;1:71–82.
7 Chan SC: Liver transplantation for hepatocellular carcinoma. Liver Cancer 2013;2:338–344.
8 Kudo M: Japan's successful model of nationwide hepatocellular carcinoma surveillance highlighting the urgent need for global surveillance. Liver Cancer 2012;1:141–143.
9 Lin SM: Local ablation for hepatocellular carcinoma in Taiwan. Liver Cancer 2013;2:73–83.
10 Bedossa P, Carrat F: Liver biopsy: the best, not the gold standard. J Hepatol 2009;50:1–3.
11 Masuzaki R, Tateishi R, Yoshida H, Yoshida H, Sato S, Kato N, Kanai F, Sugioka Y, Ikeda H, Shiina S, Kawabe T, Omata M: Risk assessment of hepatocellular carcinoma in chronic hepatitis C patients by transient elastography. J Clin Gastroenterol 2008;42:839–843.
12 Masuzaki R, Tateishi R, Yoshida H, Goto E, Sato T, Ohki T, Imamura J, Goto T, Kanai F, Kato N, Ikeda H, Shiina S, Kawabe T, Omata M: Prospective risk assessment for hepatocellular carcinoma development in patients with chronic hepatitis C by transient elastography. Hepatology 2009;49:1954–1961.
13 Jung KS, Kim SU, Ahn SH, Park YN, Kim do Y, Park JY, Chon CY, Choi EH, Han KH: Risk assessment of hepatitis B virus-related hepatocellular carcinoma development using liver stiffness measurement (fibroscan). Hepatology 2011;53:885–894.
14 Fujimoto K, Wada S, Oshita M, Kato M, Tonomura A, Mitake T: Non-invasive evaluation of hepatic fibrosis in patients with chronic hepatitis C using elastography. Medix 2007;(suppl):24–27.
15 Tatsumi C, Kudo M, Ueshima K, Kitai S, Takahashi S, Inoue T, Minami Y, Chung H, Maekawa K, Fujimoto K, Akiko T, Takeshi M: Noninvasive evaluation of hepatic fibrosis using serum fibrotic markers, transient elastography (FibroScan) and real-time tissue elastography. Intervirology 2008;51(suppl 1):27–33.
16 Shiina T, Maki T, Yamakawa M, Mitake T, Kudo M, Fujimoto K: Mechanical model analysis for quantitative evaluation of liver fibrosis based on ultrasound tissue elasticity imaging. Jpn J Appl Phys 2012;51:1–8.
17 Fujimoto K, Kato M, Tonomura A, Yada N, Tatsumi C, Oshita M, Wada S, Ueshima K, Ishida T, Furuta T, Yamasaki M, Tsujimoto M, Motoki M, Mitake T, Shiina T, Kudo M, Hayashi N: Non-invasive evaluation method of the liver fibrosis using real-time tissue elastography – usefulness of judgment liver fibrosis stage by liver fibrosis index (LF index) (in Japanese). Kanzo 2010;59:539–541.
18 Fujimoto K, Kato M, Kudo M, Yada N, Shiina T, Ueshima K, Yamada Y, Ishida T, Azuma M, Yamasaki M, Yamamoto K, Hayashi N, Takehara T: Novel image analysis method using ultrasound elastography for non-invasive evaluation of hepatic fibrosis in patients with chronic hepatitis C. Oncology 2013;84(suppl 1):3–12.
19 Yada N, Kudo M, Morikawa H, Fujimoto K, Kato M, Kawada N: Assessment of liver fibrosis with real-time tissue elastography in chronic viral hepatitis. Oncology 2013; 84(suppl 1):13–20.
20 Kudo M, Shiina T, Moriyasu F, Iijima H, Tateishi R, Yada N, Fujimoto K, Morikawa H, Hirooka M, Sumino Y, Kumada T: JSUM ultrasound elastography practice guidelines: liver. J Med Ultrason 2013;40:325–357.
21 Ichida F, Tsuji T, Omata M, Ichida T, Inoue K, Kamimura T, Yamada G, Hino K, Yokosuka O, Suzuki H: New Inuyama classification; new criteria for histological assessment of chronic hepatitis. Int Hepatol Commun 1996;6:112–119.
22 Tatsumi C, Kudo M, Ueshima K, Kitai S, Ishikawa E, Yada N, Hagiwara S, Inoue T, Minami Y, Chung H, Maekawa K, Fujimoto K, Kato M, Tonomura A, Mitake T, Shiina T: Non-invasive evaluation of hepatic fibrosis for type C chronic hepatitis. Intervirology 2010;53:76–81.
23 Shiina T: JSUM ultrasound elastography practice guidelines: basics and terminology. J Med Ultrason 2013;40:309–323.

結節性再生性過形成 nodular regenerative hyperplasia（NRH）の病理

鹿毛政義[*1] 近藤礼一郎[*1]

索引用語：結節性再生性過形成，NRH，特発性門脈圧亢進症，partial nodular transformation，門脈圧亢進症

1 はじめに

肝臓には種々の過形成性結節性病変がみられる．その中で代表的な病変は，限局性結節性過形成Focal nodular hyperplasia（FNH）であるが，FNHの他にも結節性再生性過形成nodular regenerative hyperplasia（NRH）[1-8]や部分的結節性形成性変化partial nodular transformation（PNT）[9,10]がある．これらの過形成性結節性病変は，非硬変性門脈圧亢進症と呼ばれる疾患，すなわち特発性門脈圧亢進 症idiopathic portal hypertension（IPH），肝外門脈閉塞症，先天性門脈欠損症，Budd-Chiari症候群などにみられる[11]．これらの疾患に共通する病態は，肝臓内の門脈や肝動脈の血行動態の異常に起因することであり，しばしば門脈圧亢進症を伴う．過形成性結節性病変は，近年の画像診断技術の進歩や超音波誘導下針生検の普及と相まって発見される機会が多くなった[12,13]．しかし本邦では非硬変性門脈圧亢進症は稀であり，随伴する過形成性結節性病変については十分には明らかにされていない．

本稿では，NRHについて概説するとともに，NRHを合併するIPHさらにPNTの臨床病理像について説明を行い，過形成性結節性病変について整理を試みたい．

2 NRH

1．概念

NRHは1959年にSteiner[2]が提唱した病理学的概念で，その特徴はびまん性に生じる肝細胞の過形成からなる小結節形成で，個々の結節は肝小葉より小さなものが多い．NRHが肝硬変と異なる点は，肝硬変でみられる結節を取り囲む線維性隔壁を欠くことである．このような病変は，miliary hepatocellular adenomatosis，nodular transformation of the liv-

Masayoshi KAGE et al：Pathology of nodular regenerative hyperplasia
[*1] 久留米大学病院病理診断科・病理部［〒830-0011 福岡県久留米市旭町67］

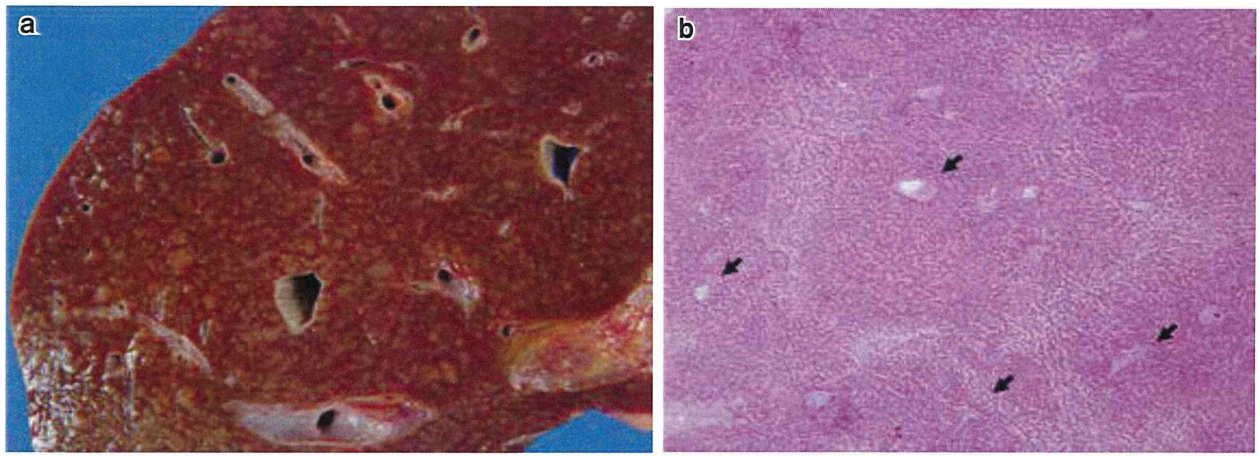

図1

a：NRHの肝肉眼像．割面全体に小結節が観察される．
b：Aの組織像．末梢門脈域(矢印)を中心に肝細胞の小さな過形成結節がびまん性に認められる．結節間には肝硬変でみられるような線維性隔壁はない(HE染色，×12.5)．

er, nodular non-cirrhotic liver, non-cirrhotic nodulationなどさまざまな用語で表現されてきた．

2. 臨床的事項

主に成人にみられ，小児は稀である．性差はやや女性に多い．NRHは通常，全身性疾患に合併して生じる[2-8]．Steiner[2]は非代償性の心不全によるうっ肝でNRHを見いだしているが，ほかにも種々の疾患で観察される．IPH[8,11]，Felty症候群[6]，関節リウマチ，全身性紅斑性狼瘡，CRST症候群，結節性多発動脈炎などの自己免疫疾患の頻度が高いが，真性多血症，リンパ増殖性疾患，血液疾患[7]，うっ血性心不全[2]，糖尿病，原発性胆汁性肝硬変症などNRHの基礎疾患は多様である．臨床的には無症状に経過し，剖検時偶然発見される場合と，門脈圧亢進を伴い食道静脈瘤の破裂をきたす症例や脾機能亢進を呈する症例もある．生化学的検査では肝機能の異常はないか，あっても軽度である．

3. 病理所見

NRHの疾患概念は，肝病理形態に基づく単純明快なものである．しかし，今までNRH症例として報告された肝病理形態は，実際には多様であり，結節形成が必ずしもびまん性でない症例や，結節の大きさが不均一性な症例，すなわちSteiner[2]の基準に合わない症例もNRHとみなされている．

4. 肉眼所見

NRHの典型的肉眼像は，肝表面は微細顆粒状で，割面では，肝臓全体にわたり，大きさは均一で，約3 mmの白色または黄白色の結節がびまん性に存在し，一見肝硬変に類似する(図1a)．注意深く観察すると結節の中央には点状にみえる末梢門脈域が存在する．

5. 組織所見

肝小葉構築は認識される．結節は末梢の門脈域を中心に形成されることが多く，結節の大きさは比較的均一で小さく，本来の肝小葉より小さい，すなわち亜小葉性の結節として認識される(図1b)．結節を構成する肝細胞は，肝細胞策が2～3層に厚くなり，配列はやや不規則となる．肝細胞は淡明な胞体を有し，核には異型や大小不同はない．結節周囲の肝細胞索は圧迫萎縮し，肝細胞索が結節に対して平行に配列し，類洞は拡張することが

多い．結節間には線維性隔壁はなく，この点，肝硬変とは異なる．門脈域には線維化はないか，あっても軽度である．門脈の3つ組の変化は，著変のない症例もあるが，例えばIPHでは末梢門脈枝の潰れがみられるなど．背景疾患により異なる．

6. NRHの門脈圧亢進の機序

門脈圧亢進症の発生機序として，過形成結節による肝静脈および類洞の圧排，あるいは門脈系の閉塞性変化による門脈血流の抵抗の増加を重視する報告など諸説がある[2-7]．しかし，NRHでは肝全体にびまん性に多数の結節形成が存在するにもかかわらず，すべての症例に門脈圧亢進がみられるわけではないことから，肝静脈枝の圧迫のみではNRHの門脈圧亢進を説明することは困難である．

7. 門脈圧亢進とNRHの病理像の特徴

門脈圧亢進の有無でNRHの病理所見をまとめてみると，1)門脈圧亢進を呈するNRHは，肝臓の萎縮がみられる症例が多く，このような症例では，門脈枝の潰れや系統的硬化など門脈系に異常が観察されるなど，IPHに類似する．2)門脈圧亢進を呈するNRHは，門脈圧亢進を伴わないNRHと比べて，末梢門脈枝の潰れの頻度が高い．3)ただし，門脈圧亢進を呈したNRH症例には，肝臓がむしろ腫大し，組織学的には，門脈域に顕著な変化がなく，末梢門脈枝が開存している症例もある．4)門脈圧亢進のない剖検症例で，肝臓に肉眼的に結節が認識されなくても，組織学的にNRH様所見をみることがある．

NRHを独立した疾患として捉える見方ではなく，肝内血行異常に基づく2次的な組織変化にすぎないと捉える考えもある．

3 IPHとNRH

1. IPHの概念

IPHは，脾腫，貧血，門脈圧亢進症状を主な症状とし，しかも原因となるべき肝硬変，肝外門脈・肝静脈閉塞，血液疾患などを証明しえない疾患と定義されている[1]．

2. 疫学

IPHもしくはIPH類似疾患は，米国ではhepatoportal sclerosis，インドではnon-cirrhotic portal fibrosis NCPFなど，さまざまな国から報告されている．インドなどの発展途上国に多く，欧米では少なく，本邦はそのほぼ中間と推定されている．

3. 病因

病因はいまだ不明である．歴史的には，肝原説，脾原説など諸説が提唱されて今日に至っている．現在では，細菌などの持続感染により，肝臓と脾臓の両臓器をターゲットとした，免疫反応を含めた生体反応が生じ，その結果，肝内門脈が傷害され潰れ，脾臓には，うっ血だけでは説明できない巨脾を惹起させるのではないかと推察されている．

4. 基本的な肝病理形態[1]

1）肉眼所見

剖検肝では萎縮が目立つ症例が多く，肝重量が約600 gの症例などもある．また右葉ないしは左葉の極端な萎縮がみられる(図2a, b)症例がある．このような症例では，肝門部門脈主幹に新旧の血栓による閉塞が観察される．肝表面にはしばしば皺壁が観察される．

2）病理組織所見

末梢門脈枝の潰れや肝内門脈枝の系統的硬化と血栓形成などが特徴とされるが，結節性変化もみられる症例もあり，その組織像は多彩である．

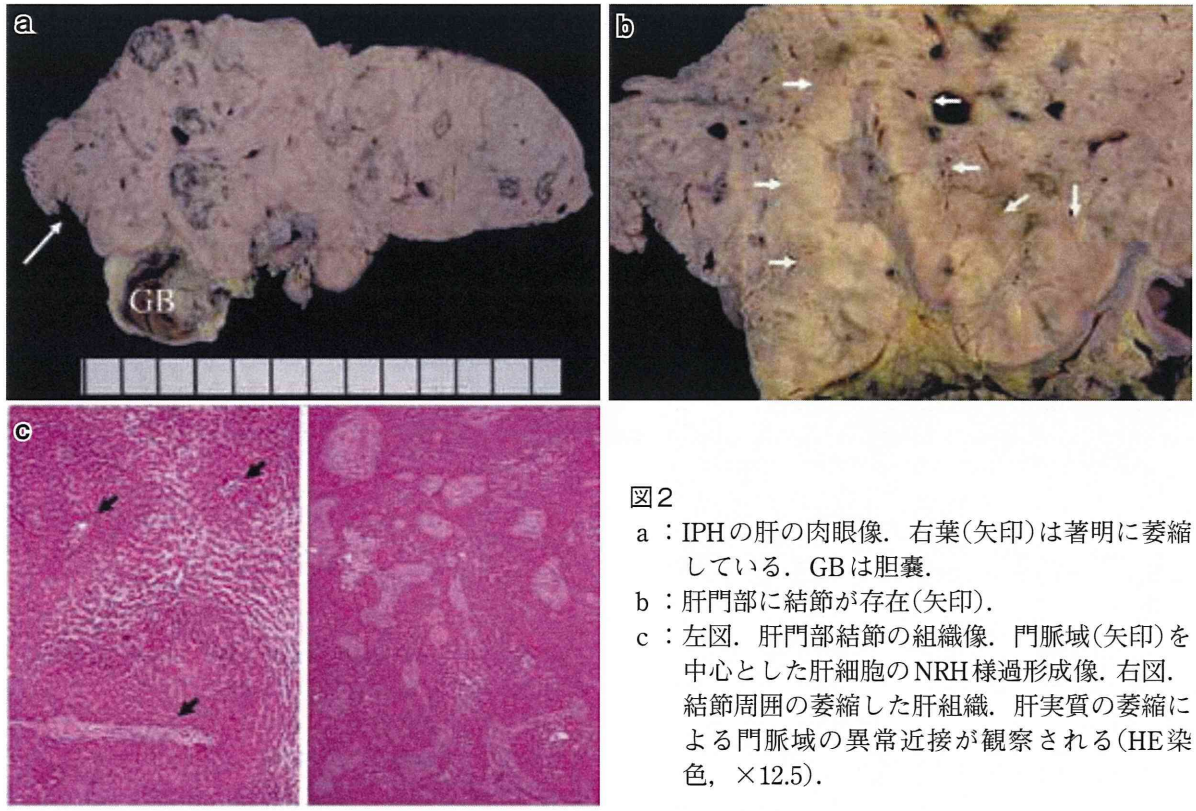

図2
a：IPHの肝の肉眼像．右葉(矢印)は著明に萎縮している．GBは胆嚢．
b：肝門部に結節が存在(矢印)．
c：左図．肝門部結節の組織像．門脈域(矢印)を中心とした肝細胞のNRH様過形成像．右図．結節周囲の萎縮した肝組織．肝実質の萎縮による門脈域の異常近接が観察される(HE染色，×12.5)．

5. 肝の結節性変化の病理学的特徴

1) 結節の分布

結節は，主に肝門部や中等大門脈域の周囲にみられる(図2b)が，肝被膜下領域に形成されることもある．

6. 結節の病理形態

1) 肉眼像

結節の大きさは，形状は，色調は，白色から黄白色調を呈することが多く，周囲肝組織と比べて白っぽい，淡明な色調を呈する．

2) 組織像

肉眼では明瞭に観察された結節でも，組織では，境界が意外と不明瞭で，結節として認識しがたいことが，しばしばである．平易に表現すると，組織上では結節の輪郭の線引きがしにくい．結節に被膜を伴うことは通常ない．結節は肝細胞の過形成であり，肝細胞索が2～3層に厚くなり，配列はやや不規則となり，肝細胞は淡明な胞体を有し，核には異型性はみられない．末梢門脈域を中心にこれらの肝細胞の過形成が小結節を形成し，NRHの所見を呈することもある(図2c左図)．過形成の周囲には萎縮した肝実質が存在し，異常な門脈域間の近接をみる(図2c右図)．

7. IPHの結節形成機序

IPHにみられる肝門部の肝細胞の過形成性変化の機序については十分には明らかにされていない．門脈血行障害の結果，脱落した肝被膜下領域の肝実質の脱落に対し，これを代償するように肝血流の保持された肝門部に肝細胞の過形成が生じる可能性がある．

8. 結節を伴うIPHとNRHとの異同

1) IPH肝に肉眼的に認識される結節性病変は，組織学的には，肝細胞の過形成性病変であり，NRH様の所見を呈することがある．

2) Steiner[2]の古典的なNRHと異なる点は，IPHでは結節の大きさが不均一で，肝臓全体にびまん性にみられない点である．

3) しかし，IPH症例でも結節が多発して観察されることがある．IPHの診断基準を満た

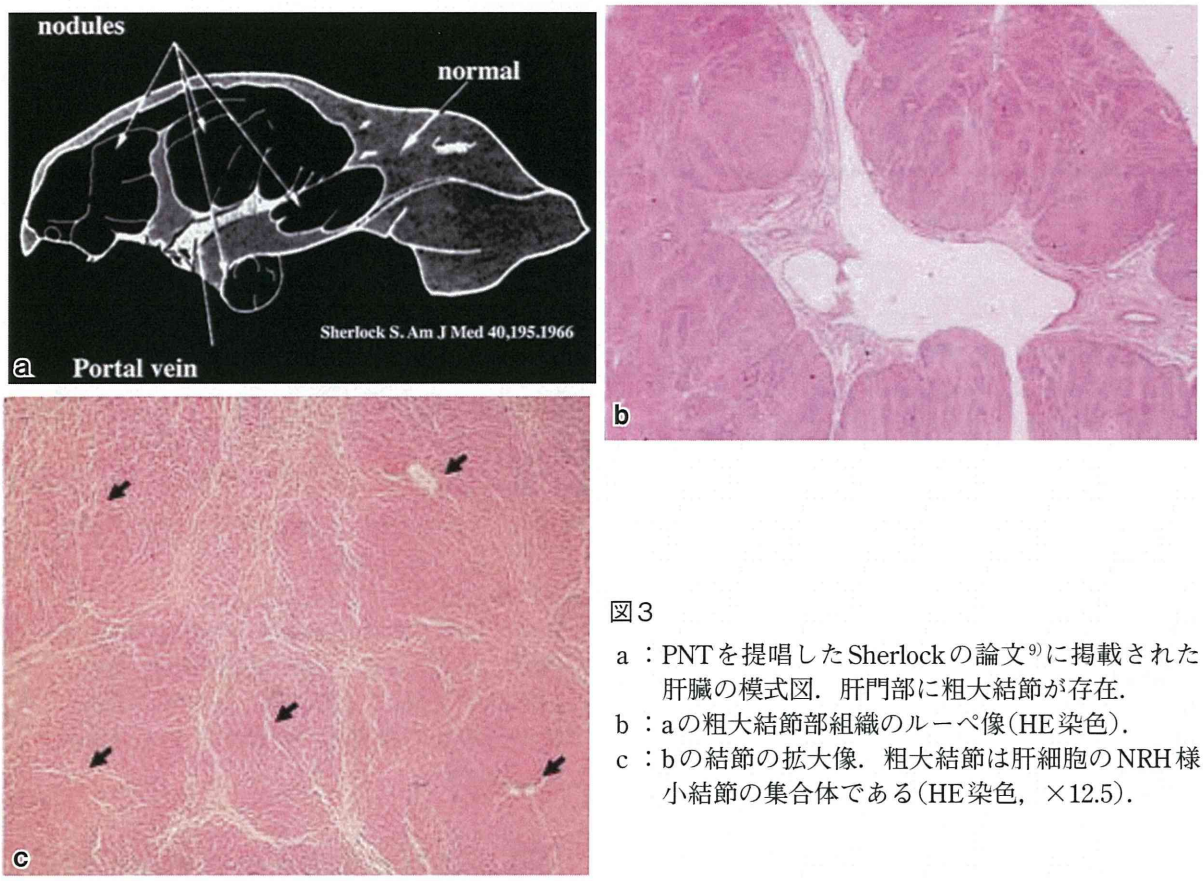

図3
a：PNTを提唱したSherlockの論文[9]に掲載された肝臓の模式図．肝門部に粗大結節が存在．
b：aの粗大結節部組織のルーペ像(HE染色)．
c：bの結節の拡大像．粗大結節は肝細胞のNRH様小結節の集合体である(HE染色，×12.5)．

し，かつ，NRH様所見がみられる症例は，「NRH様過形成結節を伴うIPH」と表現するのが妥当と考える．

4 PNTとNRH

1. PNTの概念

PNTは，1966年Sherlockら[9]によって初めて記載された疾患で，肝臓の2/3以上を占拠する肝門部に大きな結節を有し，脾腫と食道静脈瘤を伴う門脈圧亢進を示す疾患である．

2. 病因

不明である．内外において，PNTの症例報告は少なく，その病態および門脈圧亢進の発生機序の解明は遅れている．IPHあるいはNRHとの異同が論議される中，PNTの疾患としての独立性にも疑問が持たれているのが現状である．

3. 臨床的事項

中年女性に多い傾向にある．門脈圧亢進症とそれに伴う吐血，下血および貧血があり，腹水も時に観察される．肝機能検査は正常かやや機能低下している．

4. 基本的な肝病理形態

1）肉眼所見

肝重量は，ほぼ正常かやや萎縮する．肝表面は時に突出するように結節状に隆起する．割面は，周囲をやや圧排するように，肝門部を中心に直径6～8 cmの大結節を形成する．肝被膜下領域は正常もしくは萎縮が観察される．

2）組織所見

結節部は肝細胞の過形成性変化であり，NRH様の過形成性結節が集合したものであった．門脈域を中心として異型のない肝細胞が索状に2～3層に配列する．

筆者は，Sherlockら[9]が報告したPNTの標

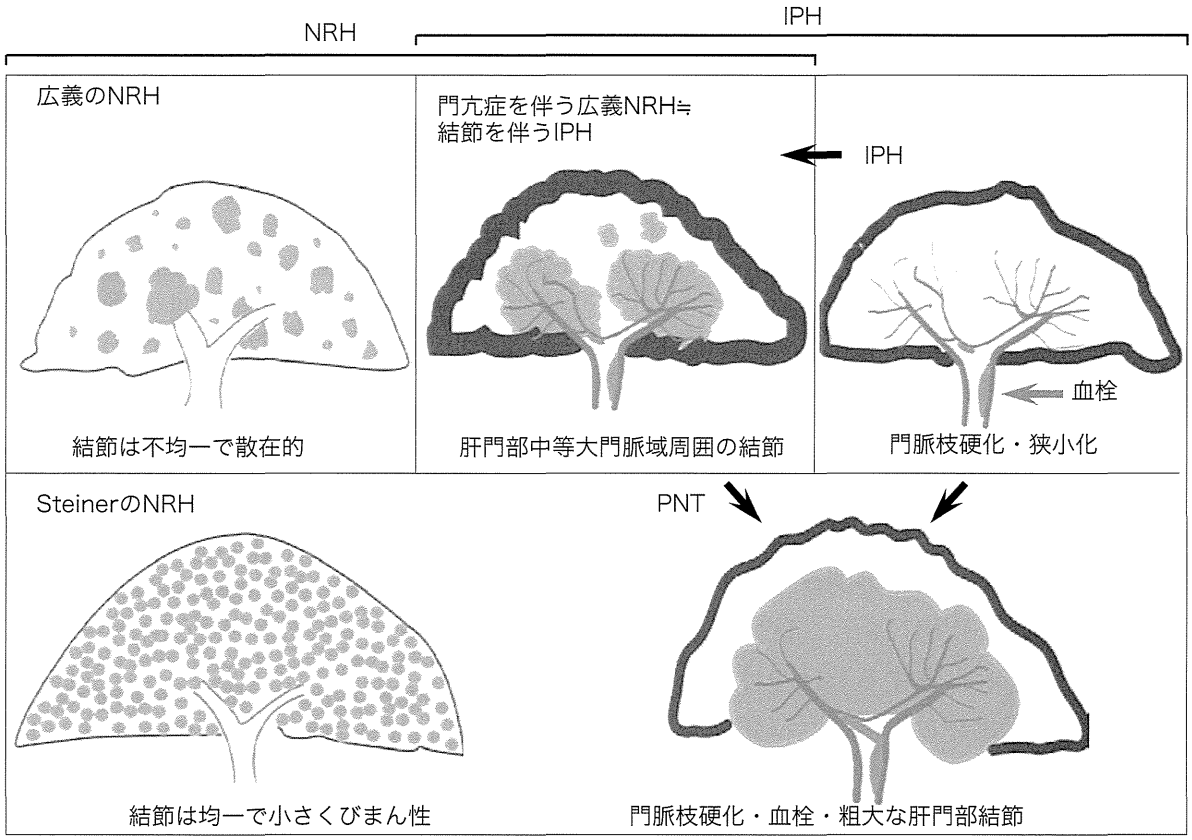

図4　肝に過形結節を呈するIPH，NRHおよびPNTを肝病理形態の比較

本を鏡検する機会があったので，少し，病理組織所見を付け加える．非結節部では，IPHと類似する組織所見が多かった．例えば，IPHの病理形態の特徴とされる肝末梢門脈枝の潰れ，被膜下領域の肝実質の萎縮，門脈域の円形の線維性拡大，末梢門脈枝の潰れや狭小化，中等大および門脈主幹にわたる系統的門脈硬化が観察された．

5. PNTとIPHの類似性

Shedlofskyら[14]は，21歳，男性の門脈圧亢進と出血性静脈瘤を有する例で，病理学的にPNTとNRHの両方の所見がみられ，血管造影ではIPHに類似した所見を呈した症例を報告している．筆者らは，PNTとIPHとの病理形態の異同を客観的に評価するため，IPHの剖検肝と典型的なPNTの肉眼像を呈した剖検肝を対象に，コンピューター画像解析装置を用い肝内脈管の内腔面積の組織計測を行った[10]．その結果，PNTは肝門部領域，肝被膜下領域ともに末梢門脈枝内腔は狭小化していたが，肝動脈枝は両領域においてほぼ正常に開存していた．IPH肝との比較では，門脈枝内腔の狭小化がみられる点はPNTと一致したが，IPH肝は肝動脈枝の内腔面積が，肝被膜下領域と肝門部領域ともに，狭小化していた．

6. PNTの結節形成機序－PNTはIPHの亜型か？

このPNT症例にみられた肝門部の過形成性変化の機序は不明であるが，肝動脈血流が維持されていた肝門部領域において，肝被膜下領域の萎縮に対する代償性の過形成変化が生じた可能性が推察された．IPHの肝との病理形態の類似性から，末梢門脈枝の狭小化や潰れによる門脈血流抵抗の上昇が惹起された可能性が推測された．PNTとIPHとの肝病

理形態の類似性をもって，両者を安易に同一視することは避けねばならないが，PNTは，肝門部に異常に大きな結節を形成したIPHの亜型かもしれない．

以上，PNTとIPHとの肝病理形態の類似性を強調したが，PNTの症例報告の中には，IPHに特徴とされる肝病理所見を欠く症例も存在するようである．

7. NRH，結節を伴うIPHおよびPNTの関係について

図4にNRH，PNT，IPHの病理形態の特徴と結節形成と門脈圧亢進との関係を模式的に示した．それぞれの疾患に相互に区別しうる特異的な病理所見が存在するわけではなく，肉眼および組織変化がともに相互に類似する点が多いことに注目してもらいたい．NRH，PNTおよびIPHの臨床および病理学的所見がしばしば，オーバーラップして観察される．

5 おわりに

NRHならびに肝に同様の過形成変化を呈するIPHとPNTについて概説した．これらの疾患にみられる肝細胞の過形成は，肝内の血行異常を背景に発生すると推測されているが不明な点は多い．NRHなど肝の良性の結節性病変に対する疾患概念や名称については統一されていないのが現状であり，その発生機序や病態をふまえた疾患概念の整理が望まれる．そのためには，症例を集積し集学的な検討を行いコンセンサスを得ることが必要であろう．

謝辞：長崎医療センター臨床検査科病理 黒濱大和先生，伊東正博先生に貴重なNRHの症例をご提供いただき感謝申し上げます．

文　献

1) 日本門脈圧亢進症食道静脈瘤学会編：門脈圧亢進消取り扱い規約，第3版IV病理．金原出版，東京，2013，p28
2) Steiner PE : Nodular regenerative hyperplasia of the liver. Am J Pathol 35 : 943–953, 1959
3) Wanless IR : Micronodular transformation (nodular regenerative hyperplasia) of the liver: a report of 64 cases among 2,500 autopsies and a new classification of benign hepatocellular nodules. Hepatology 11 : 787–797, 1990
4) Nakanuma Y : Nodular regenerative hyperplasia of the liver: Retrospective survey in autopsy series. J Clin Gastroenterol 12 : 460–465, 1990
5) Stromeyer FW, Ishak KG : Nodular transformation (nodular regenerative hyperplasia) of the liver-A clinico-pathologic study of 30 cases. Hum Pathol 12 : 60–71, 1981
6) Blendis LM, Parkinson MC, Shilkin KB et al : Nodular regenerative hyperplasia of the liver in Felty's Syndrome. Quart J Med 169 : 25–32, 1974
7) Wanless IR, Goldwin TA, Allen F et al : Nodular regenerative hyperplasia of hematologic disorders: A possible response to obliterative portal venopathy-A morphometric study of nine cases with hypothesis on the pathogenesis. Medicine 59 : 367–379, 1980
8) 鹿毛政義，中島　収：結節性再生性過形成およびその他の結節性病変．病理と臨床13：1390–1398，1995
9) Sherlock S, Feldman CA, Moran B et al : Partial nodular transformation of the liver with portal hypertension. Am J Med 40 : 195–203, 1966
10) 鹿毛政義，荒川正博，福田一典，他：肝のpartial nodular transformationの1例．肝臓31：777–783，1990
11) 荒川正博，鹿毛政義，福田一典，他：肝の過形成性病変と門脈圧亢進に関する病理形態学的検討．肝臓31：184–189，1990
12) 中正恵二，西上隆之，印藤克彦，他：肝結節性病変と肝内血行異常との関連についての検討．肝胆膵26：665–663，1993
13) 山田有則，高橋康二，油野民雄，他：結節性再生性過形成(NRH)画像診断21：65–67，2001
14) Shedlofsky S, Koehler RE, DeSchryver-Kecskemeti K et al : Noncirrhotic nodular transformation of the liver with portal hypertension:clonical,angiographic pathological correlation. Gastroenterology 79 : 938–943, 1980

J Hepatobiliary Pancreat Sci (2014) ••:••–••
DOI: 10.1002/jhbp.177

ORIGINAL ARTICLE

Therapeutic efficacy of splenectomy is attenuated by necroinflammation of the liver in patients with liver cirrhosis

Reiichiro Kondo · Masayoshi Kage · Toshiro Ogata · Osamu Nakashima · Jun Akiba · Yoriko Nomura · Hirohisa Yano

Abstract

Background Splenectomy is a therapy for thrombocytopenia caused by hypersplenism with liver cirrhosis. However, the determinant of therapeutic outcomes for this complication has not yet been fully clarified.

Methods We studied the laboratory findings of 55 patients who underwent splenectomy for hypersplenism with liver cirrhosis. In addition, we examined the histopathological findings of hepatosplenic tissues of nine patients who underwent hepatectomy for hepatocellular carcinoma and splenectomy for hypersplenism with liver cirrhosis on one stage surgery. The locations of platelets in hepatosplenic tissues were identified by immunohistochemistry. We used monoclonal antibody against CD41.

Results Among 55 patients, 40 patients had high serum alanine aminotransferase (ALT) level (≧38 IU/l). Blood platelet count after splenectomy of patients with high serum ALT level were significantly lower than those of patients with low serum ALT level ($P = 0.02$). Histopathologically, platelet area of the liver tissues was positively correlated with hepatic inflammation ($P = 0.02$). Platelet area of the liver tissues was negatively correlated with blood platelet count after splenectomy ($P = 0.03$).

Conclusions Hepatic inflammation contributes to the accumulation of platelets in liver; therefore, in patients with high serum ALT level, improvement of thrombocytopenia by the elimination of hypersplenism was limited.

Keywords Alanine aminotransferase · Hepatitis C · Hypersplenism · Immunohistochemical analysis · Platelet

R. Kondo (✉) · J. Akiba · Y. Nomura · H. Yano
Department of Pathology, Kurume University School of Medicine, 67 Asahi-machi, Kurume, Fukuoka 830-0011, Japan
e-mail: kondou_reiichirou@kurume-u.ac.jp

R. Kondo · M. Kage
Cancer Center, Kurume University Hospital, Kurume, Fukuoka, Japan

R. Kondo · M. Kage · Y. Nomura
Department of Diagnostic Pathology, Kurume University Hospital, Kurume, Fukuoka, Japan

T. Ogata
Department of Surgery, Kurume University School of Medicine, Kurume, Fukuoka, Japan

O. Nakashima
Department of Clinical Laboratory Medicine, Kurume University Hospital, Kurume, Fukuoka, Japan

Introduction

Cirrhosis is a major cause of morbidity and mortality in many countries, and it results in liver failure, portal hypertension, and increased risk of carcinogenesis. In chronic hepatitis, the blood platelet decreased gradually to be reflected in the liver fibrosis. Thrombocytopenia is a marked feature of liver cirrhosis. Thrombocytopenia is of great relevance in the management of liver cirrhosis because of the widespread use of myelodepressant drugs such as interferon or antineoplastic agents. However, there is no standard therapy for this complication.

The role of platelets in the pathogenesis of liver damage and exact mechanisms leading to thrombocytopenia in liver cirrhosis has not yet been fully clarified. The platelet kinetics of patients with chronic liver disease are not well characterized. The mechanisms leading to thrombocytopenia with liver cirrhosis are most likely multifactorial processes combining increased splenic platelet breakdown [1–3], splenic pooling [4, 5], and the inability of the bone marrow to increase platelet production adequately [6].

In a recent study, we reported that the accumulation of platelets in the liver may be an important contributory factor

to thrombocytopenia in chronic hepatitis C [7]. Platelets in non-cancerous liver tissues of patients with chronic hepatitis or cirrhosis were seen predominantly in the sinusoidal space of the periportal area with inflammation. As viewed through an electron microscope, the platelets were aggregated in the sinusoids and adhered to the sinusoidal endothelial cells. Platelets may accumulate in the sinusoidal space under thombocytotic conditions in chronic hepatitis C brought about by the activated hepatic reticuloendothelial system caused by inflammation [7].

Splenectomy [8, 9] and partial splenic arterial embolization [10] are therapies for thrombocytopenia caused by hypersplenism with liver cirrhosis. The elimination of hypersplenism by splenectomy or partial splenic arterial embolization improves thrombocytopenia. The spleen and chronic liver disease are closely related. In this study, we evaluated the efficacy and determinant of therapeutic outcomes of splenectomy in the treatment of thrombocytopenia caused by hypersplenism with liver cirrhosis and investigated the interaction among the liver, spleen, and blood platelets in patients with liver cirrhosis.

Methods

Materials

We studied the laboratory findings of 55 patients who underwent splenectomy for thrombocytopenia caused by hypersplenism with hepatitis C viral infection associated liver cirrhosis at Kurume University Hospital between January 2005 and December 2012. There were 30 men and 25 women. The mean age was 60 ± 8 years (range, 42 to 77 years). In addition, we examined the histopathological findings of hepatosplenic tissues of nine patients with hepatitis C viral infection associated liver cirrhosis who underwent hepatectomy for hepatocellular carcinoma and splenectomy for hypersplenism on one stage surgery at Kurume University Hospital between January 1999 and December 2007. There were three men and six women. The mean age of patients was 59 ± 9 years (range, 41 to 70 years). Five specimens of liver tissue and nine specimens of splenic tissue without chronic hepatitis or thrombocytopenia that were obtained during surgery were used as normal control tissues.

Splenectomy was generally performed in hypersplenic patients with thrombocytopenia (platelet count $< 6 \times 10^4/mm^3$) or leukopenia (white blood cell count <3000 /μl). All patients did not receive myelodepressant drugs or preoperative anticancer therapies and there were no postoperative complications such as severe infection.

This study was performed with informed consent obtained from patients for the use of their laboratory data, liver tissues and splenic tissues in the investigation and was approved by the Ethical Committee at Kurume University, the approved ID number: 11 200.

Laboratory study

Blood samples of all patients were collected from a peripheral vein of the extremities before surgery and 3 months after. We estimated blood cell count, serum alanine aminotransferase (ALT) level, serum total bilirubin level, serum albumin level, and prothrombin time.

Histopathology

Non-cancerous liver tissues and splenic tissues from nine patients who underwent hepatectomy and splenectomy on one stage surgery were obtained during surgery. Each tissue, fixed with 10% formalin embedded in paraffin, and cut into 5-μm sections, was used for histological and immunohistochemical analyses. Specimens were stained with hematoxylin and eosin and examined under a light microscope.

The histologic liver damage of these specimens was evaluated for fibrosis and inflammation according to the classification proposed by the International Association for the Study of the Liver [11, 12]. The severity of fibrosis was classified as none: stage 0, portal fibrosis: stage 1, periportal fibrosis: stage 2, bridging fibrosis with lobar distortion: stage 3, and cirrhosis: stage 4. The inflammatory activity was classified as none: grade 0, minimal: grade 1, mild: grade 2, moderate: grade 3, or severe: grade 4. Histopathological diagnosis was performed by three pathologists (RK, ON and MK).

Immunohistochemical analysis

An immunohistochemical study was performed using the streptavidin-biotin method. We used monoclonal antibody against CD41 (1:500, Beckman Coulter, Brea, CA, USA). 3, 3'-diaminobenzidine (DAB) was used as the chromogen in the immunostaining. CD41 (α II b integrin) is a specific marker for platelets [13]. Among CD41-positive cells, those without nuclei were evaluated as platelets and those with large, irregular shaped nuclei were evaluated as megakaryocytes.

Measurement of cells

The platelet area was measured using a WinROOF software package (version 6.1, Mitani Corporation, Fukui, Japan). In liver tissues, the platelet area was measured in five

Table 1 Clinical features of 55 patients with splenectomy

	Before splenectomy	3 months after splenectomy	*P*-value
Blood white cell count (/μl)[a]	2,960 ± 1,236 (1,100–8,200)	4,965 ± 1,859 (2,400–11,100)	<0.01
Blood red cell count (/μl)[a]	393 ± 51 (306–520)	387 ± 49 (288–503)	0.56
Blood platelet count ($\times 10^4/mm^3$)[a]	4.4 ± 1.5 (1.4–7.7)	17.5 ± 7.6 (6.1–47.4)	<0.01
ALT (IU/l)[a]	55 ± 24 (18–157)	42 ± 16 (15–91)	<0.01
T. bil (mg/dl)[a]	1.4 ± 0.7 (0.5–4.8)	1.1 ± 0.5 (0.4–2.9)	<0.01
PT (%)[a]	72 ± 12 (49–94)	66 ± 15 (36–96)	0.04
Alb (g/dl)[a]	3.5 ± 0.4 (2.4–4.5)	3.5 ± 0.5 (2.3–4.6)	0.77

Alb serum albumin level, *ALT* serum alanine aminotransferase level, *PT* prothrombin percentage activity, *T.bil* serum total bilirubin level
[a]Mean ± SD (range)

Table 2 Comparison of preoperative patient characteristics based on therapeutic effect of splenectomy

	Limited response group (n = 30)	Response group (n = 25)	*P*-value
Gender (male / female)	16 / 14	9 / 16	0.2
Age (years)[a]	61 ± 8	60 ± 8	0.97
Blood white cell count (/μl)[a]	3,067 ± 1,396	2,832 ± 1,026	0.49
Blood red cell count (/μl)[a]	378 ± 40	412 ± 58	0.01
Blood platelet count ($\times 10^4/mm^3$)[a]	4.3 ± 1.6	4.5 ± 1.4	0.73
ALT (IU/l) (< 38 / ≧ 38)	5 / 25	10 / 15	0.05
T. bil (mg/dl)[a]	1.4 ± 0.9	1.3 ± 0.5	0.61
PT (%)[a]	75 ± 9	68 ± 13	0.04
Alb (g/dl)[a]	3.4 ± 0.4	3.6 ± 0.4	0.06

Alb serum albumin level, *ALT* serum alanine aminotransferase level, *PT* prothrombin percentage activity, *T.bil* serum total bilirubin level
[a]Mean ± SD (range)

periportal and five lobule areas randomly selected. In splenic tissues, five visual fields in the red pulp were randomly selected.

Statistical analysis

All data are expressed as the mean ±standard deviation (SD). Quartile value was determined for the measured variables. Comparisons between two groups of patients, those based on blood platelet count after splenectomy, were performed using the Mann–Whitney *U*-test for continuous variables, and χ^2 test for discrete variables. Only variables that demonstrated a *P*-value of under 0.05 in the univariate analysis were entered into a multiple logistic regression model to identify factors associated with blood platelet count after splenectomy. Pearson correlation coefficients were calculated to examine the association of blood platelet count after splenectomy and preoperative serum ALT level. *P*-values less than 0.05 were considered to indicate significance. Statistical analysis was performed using a JMP software package (Release 11.0, SAS Institute, Cary, NC, USA).

Results

Laboratory findings of 55 patients who underwent splenectomy

Summary of laboratory findings of 55 cirrhotic patients who underwent splenectomy are shown in Table 1. Blood platelet count, blood white cell count and serum total bilirubin level significantly improved 3 months after splenectomy. The mean value of blood platelet count 3 months after splenectomy was $17.5 \times 10^4/mm^3$. The mean value and quartile value of serum ALT level before splenectomy were 55 IU/l and 37 IU/l, respectively. The Response group, in which the blood platelet counts 3 months after splenectomy were over $17.5 \times 10^4/mm^3$, was 25 patients and the Limited response group, in which the blood platelet count 3 months after splenectomy was under $17.5 \times 10^4/mm^3$, was 30 patients. The preoperative characteristics of the two-patient response group are shown in Table 2. There was significant difference of blood red cell count, serum ALT level, and prothrombin time between the Response group and Limited response group.